Deterministic tuning of slow-light in photonic-crystal waveguides through the C and L bands by atomic layer deposition

Charlton J. Chen,[1,a)] Chad A. Husko,[1] Inanc Meric,[2] Ken L. Shepard,[2] Chee Wei Wong,[1] William M. J. Green,[3] Yurii A. Vlasov,[3] and Solomon Assefa[3,b)]

[1]*Optical Nanostructures Laboratory, Columbia University, New York 10027, USA*
[2]*Department of Electrical Engineering, Columbia University, New York 10027, USA*
[3]*IBM T. J. Watson Research Center, Yorktown Heights, New York 10598, USA*

We demonstrate digital tuning of the slow-light regime in silicon photonic-crystal waveguides by performing atomic layer deposition of hafnium oxide. The high group-index regime was deterministically controlled (redshift of 140 ± 10 pm per atomic layer) without affecting the group-velocity dispersion and third-order dispersion. Additionally, differential tuning of 110 ± 30 pm per monolayer of the slow-light TE-like and TM-like modes was observed. This passive postfabrication process has potential applications including the tuning of chip-scale optical interconnects, as well as Raman and parametric amplification. © *2010 American Institute of Physics*. [doi:10.1063/1.3308492]

Dramatic reduction in the group-velocity of light has been demonstrated in atomic and solid-state systems[1,2] with greatly increased light-matter interaction, although typically at the expense of bandwidth. Slow-light in photonic-crystal waveguides (PhCWGs), through strong structural dispersion, allows larger bandwidth for potential applications such as optical buffering and switching,[3,4] disordered localization,[5] and nonclassical optics.[6] The dispersion-to-loss ratio[7] is comparable to that of single-mode optical fibers, allowing strong enhancement of nonlinear processes on the chip, such as third-harmonic generation, self-phase modulation, and Raman and parametric processes.[8,9] However, in order to operate at a particular frequency, these devices often possess stringent fabrication requirements that are difficult to achieve using current e-beam or deep-UV lithography; even slight fabrication deviations at the nanometer level can shift the tight operating bandwidths of the integrated photonic devices.[10] Active approaches to tune photonic elements include aligned external pump laser beams, integrated piezo-electric elements,[11] or microheaters.[3] To maintain the shifted dispersion or resonances in active tuning approaches, a finite external power must be continuously applied to the photonic elements. Alternatively, passive tuning approaches have been examined, such as GaAs wet-etching[12] and electron beam induced compaction.[13] Recently we examined an atomic layer deposition (ALD) approach to tune PhC microcavity resonances with a precision of ~ 122 pm per hafnium oxide (HfO_2) layer.[14] Here we propose and demonstrate for the first time a passive postfabrication scheme for tuning dispersion in slow-light PhCWGs by utilizing a digital self-limiting deposition of HfO_2 monolayers.

To study the effect of passive tuning of the slow-light regime, we designed PhC waveguides and Mach–Zehnder interferometer (MZI) devices for transmission measurements in the near-infrared.[3,15] Each MZI device consists of a Y-splitter connected to a strip waveguide on one arm and to

a PhCWG on the other arm, as shown in Fig. 1(b). The interference fringes from MZI spectral measurements are used to determine group-velocity using a procedure described below. The PhCWGs are W0.9 line defects created by removing a single row of air holes in a hexagonal lattice of air holes along the Γ-K direction and then decreasing the defect width by 10%. The lattice parameter (a) is 410 nm with air hole radii of 108 nm (r/a ratio of 0.263). The structures were fabricated by e-beam lithography on silicon-ion-insulator substrates with a silicon slab thickness of 220 nm (t/a ratio of 0.537). The PhCWG is 250 μm long and butt-coupled to strip waveguides at both ends, and has previously demonstrated low-loss of 2.4 dB/mm.[16] The underlying oxide was subsequently removed by hydrofluoric acid etching. The silicon strip waveguides are tapered adiabatically as they connect to polymer couplers which are used for low-loss coupling to off-chip polarization-maintaining tapered-lensed fibers.[16]

Figure 2(a) shows the projected band structure of our PhCWG, computed through three-dimensional plane wave expansion.[17] In order to get the best fitting to experimental data a procedure described in Ref. 15 was used. Within the band gap, there are two TE-like modes (even and odd modes). The even mode exhibits slow-light characteristics near the band-edge where $d\omega/dk$ becomes increasingly small, resulting in large group indices, $n_g = c(dk/d\omega)$. The corresponding projected band structure for the TM-like mode is shown Fig. 2(b) where, although no band gap exists, one observes a Bragg stop gap due to the periodic modulation of the effective index in the propagation direction.[18]
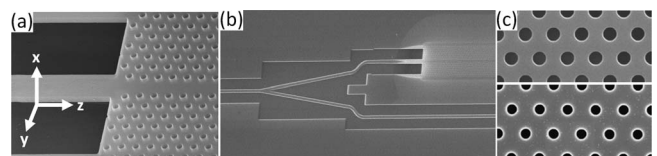

FIG. 1. SEM image of (a) PhCWG and strip waveguide interface (b) MZI structure with PhCWG on upper section and strip waveguide on lower section. (c) PhC before deposition (upper image) and after 160 ALD layers of HfO_2.

a)Author to whom correspondence should be addressed. Electronic mail: cjc2106@columbia.edu.
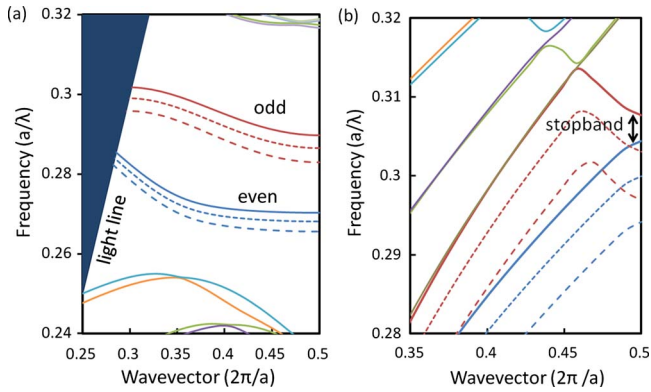b)Electronic mail: sassefa@us.ibm.com.

FIG. 2. (Color online) Band structures calculated using plane-wave expansion method. Solid-lines correspond to no HfO$_2$ deposition. Dotted-lines and dashed-lines correspond to 80 and 160 atomic layers of HfO$_2$ deposition, respectively. (a) Projected band diagram for TE-like W0.9 waveguide modes (b) Corresponding TM band diagram. Note that the vertical and horizontal ranges are different than in (a).

FIG. 3. (Color online) (a) TE transmission measurements for different ALD tuning steps. (b) Corresponding TM transmission measurements.

In order to tune the structures, sequential conformal deposition of HfO$_2$ atomic layers was performed. HfO$_2$ was chosen as the ALD material due to its wide band gap, low optical absorption,[19] and direct complementary metal-oxide semiconductor-compatibility having been used as a high-k dielectric gate insulator in the 45 nm technology node.[20] Prior to each deposition step, samples were cleaned with acetone, isopropanol, and UV ozone. The UV generated ozone was used to create a hydrophilic surface favorable for the ALD process. Monolayer films were deposited at a temperature of 200 °C using two precursors, tetrakis(diethylamido)hafnium(IV) [Hf(DEA)4] and water (H$_2$O) vapor, in alternating pulses. Nitrogen gas was flowed through the reaction chamber during the entire process. Lower temperature depositions are also possible with the trade-off of longer deposition times. The process is self-limiting and deposits one atomic layer at a time, with deposition rate of approximately 0.1 nm per minute. As shown by the SEM image in Fig. 1(c), the ALD deposited film is high quality and uniform even inside of the air holes. Because ALD is a conformal process, each cycle incrementally decreases the hole radii and increases the slab thickness. The increase in brightness around the hole after ALD deposition is due to charging effects in the HfO$_2$ during SEM imaging.

Digital tuning was performed in increments of 40 atomic layers, with 1.05 ± 0.05 Å thickness for each HfO$_2$ atomic layer.[21] After each of these deposition steps (40 atomic layers), transmission measurements were performed for both the TE and TM polarizations. Light from a supercontinuum source was coupled into the on-chip polymer couplers using a polarization-maintaining tapered-lensed fiber. The output from the chip was similarly coupled to a tapered-lensed fiber and measured with an optical spectrum analyzer in the spectral range of 1300 to 1600 nm. The measured transmission spectra were normalized by the transmission spectra through a reference strip waveguide.

Figure 3(a) shows a series of TE transmission spectra after sequential ALD deposition steps. A wide bandwidth transmission region extends across the lower wavelength range followed by a sudden drop in transmission around 1514 nm for the predeposition measurement. The slow-light regime, which is close to the onset of the waveguiding mode, is characterized by high group-indices as shown in Fig. 4(a).
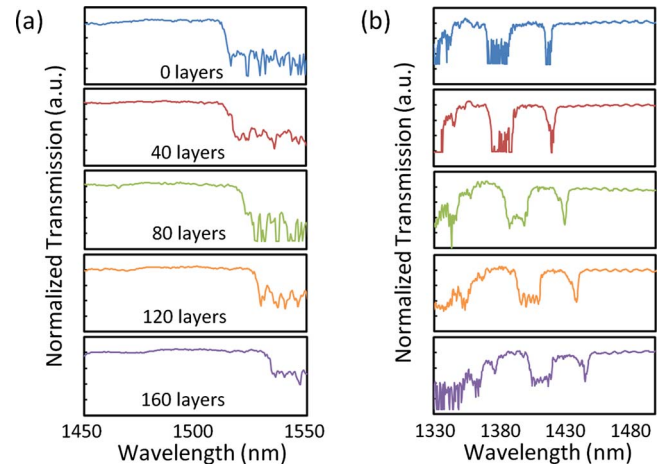
We observed a deterministic redshift in the slow-light TE-like mode onset edge from 1513.8 nm (before ALD tuning) to 1533.7 nm (after 160 ALD deposition cycles), with the slow-light edge determined by a 10 dB drop in transmission corresponding to a group index of approximately 40. The inset of Fig. 4(a) illustrates that the redshift is linear, with a 140 ± 10 pm per monolayer control of the slow-light mode onset edge. The initial deposition step was not used in calculating this value because the slow-light redshift in the first deposition step was smaller than subsequent deposition steps. This is likely due to the formation of an 8–10 Å interfacial layer between HfO$_2$ and silicon during the first 20 ALD deposition cycles.[21,22] In addition, on a different chip we have also tuned the slow-light edge across the entire optical communications C-band (and into part of the L-band), with tuning from 1530.6 to 1597.8 nm with 450 ALD cycles, i.e., 150 ± 10 pm per monolayer.[23]

Figure 3(b) shows a series of TM transmission spectra after sequential ALD deposition steps. Unlike the TE-like slow-light mode which is found in the TE band gap, the TM-like slow-light modes are found on either side of the
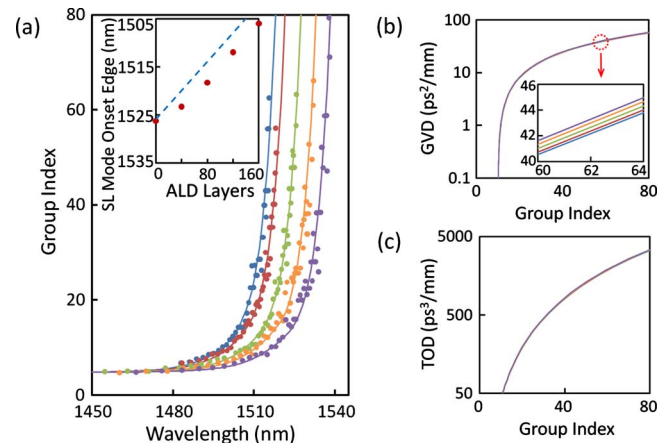

FIG. 4. (Color online) (a) Group-index measurements from MZI devices. The number of atomic layers deposited corresponds to those described in Fig. 3(a). The solid lines are provided for clarity. Inset: measured slow-light mode onset (circles) and numerical simulations (dashed line). [(b) and (c)] Group-velocity dispersion and TOD for the different ALD tuning steps. The inset is a magnified view showing the slight variation in GVD between deposition steps.

stop gap [illustrated by the dashed-lines in the computed band structure of Fig. 2(b)]. The TM-like modes are also redshifted with the ALD deposition. The redshift for the shorter-wavelength TM slow-light mode is likewise linear with control from 1370.7 to 1403.5 with 160 ALD layers, or 250 ± 10 pm per monolayer. The larger TM shift is due to the larger modal area and overlap with the HfO_2 monolayers. On comparing the slow-light tuning of the TE and TM modes, we note that there is a differential shift of 110 ± 30 pm per monolayer. This difference can be used for exact tuning of the pump-Stokes frequency spacing, in order to match the optical phonons (15.6 THz) in single-crystal silicon, for cross-polarized Raman amplification.[18]

Along with PhCWG transmission measurements, MZI transmission measurements were taken to determine group indices using a frequency-domain interferometric technique.[3,15] The MZI structure is shown in Fig. 1(b). The results of the measurements (over a total of 160 atomic layers) are summarized in Fig. 4(a). The solid lines are from exponential fitting of group indices which were in-turn deduced from the spectral positions of minima and maxima in the MZI transmission with the following: $n_g(\lambda) = \lambda_{min}\lambda_{max}/(2L(\lambda_{min}-\lambda_{max}) + n_g^{ref}$, where L is the PhCWG length.[3] Both before and after ALD controlled tuning, group indices of more than 60 were consistently obtained in our measurements.

Furthermore, higher order dispersion was also studied because of the important role it plays in pulse propagation in slow-light PhCWGs.[3,24] At low group-velocities there can be a significant increase in temporal pulse width and pulse shape asymmetry due to higher order dispersion.[25] We investigated the effects of ALD on higher order dispersion, particularly the group velocity dispersion (GVD; $\lambda^2/2\pi c$) $(\partial n_g/\partial\lambda)$ and third-order dispersion (TOD; $\lambda^2/2\pi c$) $[\partial(GVD)/\partial\lambda]$. The GVD and TOD results for the different ALD deposition steps are summarized in Figs. 4(b) and 4(c), respectively. The results show that the GVD and TOD do not change appreciably while the slow-light mode onset edge is deterministically tuned by ALD, with a variation of only 3% when determined from experimental group-index data which has been fitted. This small variation is not necessarily due to ALD tuning but can also originate in part from uncertainty in fitting the data.

The effects of ALD tuning on PhCWG propagation loss have also been considered along with the effects on spatial confinement of slow-light modes. A discussion of these topics can be found in the supplemental section.[23]

In conclusion, we have demonstrated the control of slow-light dispersion characteristics of W0.9 PhCWGs using a self-limiting monolayer precision process. High group indices were digitally tuned with sequential atomic layer depositions without increasing propagation losses. A redshift of 140 ± 10 pm per atomic layer was observed for the slow-light mode onset edge, while no appreciable change was observed in the GVD and TOD. A differential shift of 110 ± 30 pm per monolayer in slow-light tuning of the TE and TM modes was observed. This difference can be used for exact tuning of the pump-Stokes frequency spacing for Raman amplification. As a low temperature postfabrication process, the atomic layer deposition of HfO_2 is an enabling passive tuning technology for many practical chip-scale slow-light devices and modules.

[1]M. S. Bigelow, N. N. Lepeshkin, and R. W. Boyd, Science **301**, 200 (2003).
[2]M. Notomi, K. Yamada, A. Shinya, J. Takahashi, C. Takahashi, and I. Yokohama, Phys. Rev. Lett. **87**, 253902 (2001).
[3]Y. A. Vlasov, M. O'Boyle, H. F. Hamann, and S. J. McNab, Nature (London) **438**, 65 (2005).
[4]T. Baba, Nat. Photonics **2**, 465 (2008).
[5]S. Mookherjea, J. S. Park, S.-H. Yang, and P. R. Bandaru, Nat. Photonics **2**, 90 (2008).
[6]V. S. C. Manga Rao and S. Hughes, Phys. Rev. Lett. **99**, 193901 (2007).
[7]B. Jalali, D. R. Solli, and S. Gupta, Nat. Photonics **3**, 8 (2009).
[8]B. Corcoran, C. Monat, C. Grillet, D. J. Moss, B. J. Eggleton, T. P. White, L. O'Faolain, and T. F. Krauss, Nat. Photonics **3**, 206 (2009).
[9]J. F. McMillan, X. Yang, N. C. Panoiu, R. M. Osgood, and C. W. Wong, Opt. Lett. **31**, 1235 (2006).
[10]T. Barwicz, M. R. Watts, M. A. Popovic, P. T. Rakich, L. Socci, F. X. Kärtner, E. P. Ippen, and H. I. Smith, Nat. Photonics **1**, 57 (2007).
[11]C. W. Wong, P. T. Rakich, S. G. Johnson, M. Qi, H. I. Smith, E. P. Ippen, L. C. Kimerling, Y. Jeon, G. Barbastathis, and S.-G. Kim, Appl. Phys. Lett. **84**, 1242 (2004).
[12]K. Hennessy, A. Badolato, A. Tamboli, P. M. Petroff, E. Hu, M. Atatüre, J. Dreiser, and A. Imamoglu, Appl. Phys. Lett. **87**, 021108 (2005).
[13]J. Schrauwen, D. Van Thourhout, and R. Baets, Opt. Express **16**, 3738 (2008).
[14]X. Yang, C. Chen, C. A. Husko, and C. W. Wong, Appl. Phys. Lett. **91**, 161114 (2007).
[15]S. Assefa and Y. A. Vlasov, Opt. Express **15**, 17562 (2007).
[16]S. J. McNab, N. Moll, and Y. Vlasov, Opt. Express **11**, 2927 (2003).
[17]S. G. Johnson and J. D. Joannopoulos, Opt. Express **8**, 173 (2001).
[18]J. F. McMillan, M. Yu, D. L. Kwong, and C. W. Wong, Appl. Phys. Lett. **93**, 251105 (2008).
[19]M. Fadel, O. A. Azim M., O. A. Omer, and R. R. Basily, Appl. Phys. A: Mater. Sci. Process. **66**, 335 (1998).
[20]For a review, see R. L. Puurunen, J. Appl. Phys. **97**, 121301 (2005).
[21]J. C. Hackley, J. D. Demaree, and T. Gougousi, *Materials Science of High-k Dielectric Stacks-From Fundamentals to Technology*, MRS Symposia Proceedings No. 1073 (Materials Research Society, Pittsburgh, 2008), p. 1073–H04–19.
[22]R. Puthenkovilakam, Y. S. Lin, J. Choi, J. Lu, H. O. Blom, P. Pianetta, D. Devine, M. Sendler, and J. P. Changa, J. Appl. Phys. **97**, 023704 (2005).
[23]See supplementary material at http://dx.doi.org/10.1063/1.3308492 for experimental data from tuning the slow-light edge over a wider wavelength range. The supplementary material also contains an analysis of propagation loss and spatial confinement of slow-light modes.
[24]N. C. Panoiu, J. F. McMillan, and C. W. Wong, IEEE J. Sel. Top. Quantum Electron. (to be published).
[25]R. J. P. Engelen, Y. Sugimoto, Y. Watanabe, J. P. Korterik, N. Ideda, N. F. van Hulst, K. Asakawa, and L. Kuipers, Opt. Express **14**, 1658 (2006).